

See discussions, stats, and author profiles for this publication at: <https://www.researchgate.net/publication/11242991>

An International Evaluation of Holmium Oxide Solution Reference Materials for Wavelength Calibration in Molecular Absorption Spectrophotometry

ARTICLE in ANALYTICAL CHEMISTRY · AUGUST 2002

Impact Factor: 5.64 · DOI: 10.1021/ac0255680 · Source: PubMed

CITATIONS

15

READS

67

11 AUTHORS, INCLUDING:



[Joanne C. Zwinkels](#)

National Research Council Canada

62 PUBLICATIONS 321 CITATIONS

SEE PROFILE



[Flora E. Mercader-Trejo](#)

Universidad Politécnica de Santa Rosa Jáure...

28 PUBLICATIONS 103 CITATIONS

SEE PROFILE

An International Evaluation of Holmium Oxide Solution Reference Materials for Wavelength Calibration in Molecular Absorption Spectrophotometry

John C. Travis,[†] Joanne C. Zwinkels,[‡] Flora Mercader,[§] Arquímedes Ruíz,^{||} Edward A. Early,[⊥] Melody V. Smith,[†] Mario Noël,[‡] Marissa Maley,[†] Gary W. Kramer,[†] Kenneth L. Eckerle,[⊥] and David L. Duewer^{*,†}

Chemical Science and Technology Laboratory, National Institute of Standards and Technology, Gaithersburg, Maryland 20899-8394, Institute of National Measurement Standards, National Research Council Canada, Ottawa, Ontario K1A 0R6, Canada, Metals Division, Centro Nacional de Metrología, 76900 Querétaro, México, Optical and Radiometric Division, Centro Nacional de Metrología, 76900 Querétaro, México, and Physics Laboratory, National Institute of Standards and Technology, Gaithersburg, Maryland 20899-8441

Commercial spectrophotometers typically use absorption-based wavelength calibration reference materials to provide wavelength accuracy for their applications. Low-mass fractions of holmium oxide (Ho₂O₃) in dilute acidic aqueous solution and in glass matrixes have been favored for use as wavelength calibration materials on the basis of spectral coverage and absorption band shape. Both aqueous and glass Ho₂O₃ reference materials are available commercially and through various National Metrology Institutes (NMIs). Three NMIs of the North American Cooperation in Metrology (NORAMET) have evaluated the performance of Ho³⁺(aq)-based Certified Reference Materials (CRMs) under “routine” operating conditions using commercial instrumentation. The study was not intended to intercompare national wavelength scales but to demonstrate comparability of wavelength measurements among the participants and between two versions of the CRMs. It was also designed to acquire data from a variety of spectrophotometers for use in a NIST study of wavelength assignment algorithms and to provide a basis for a possible reassessment of NIST-certified Ho³⁺(aq) band locations. The resulting data show a substantial level of agreement among laboratories, instruments, CRM preparations, and peak-location algorithms. At the same time, it is demonstrated that the wavelength comparability of the five participating instruments can actually be improved by calibrating all of the instruments to the consensus Ho³⁺(aq) band locations. This finding supports the value of absorption-based wavelength standards for cali-

brating absorption spectrophotometers. Coupled with the demonstrated robustness of the band position values with respect to preparation and measurement conditions, it also supports the concept of extending the present approach to additional NMIs in order to certify properly prepared dilute acidic Ho₂O₃ solution as an intrinsic wavelength standard.

Molecular absorption spectrophotometers are used throughout the chemical and pharmaceutical industries for routine quantitative analysis. These instruments, commonly known as “ultraviolet–visible” (UV–visible) spectrophotometers, normally arrive from the factory meeting a wavelength accuracy specification that is more than adequate for typical analytical applications. Nevertheless, end users often rely upon absorption-based wavelength calibration reference materials to ensure the required—sometimes regulated—wavelength accuracy for their applications and to recalibrate the wavelength axis when needed.^{1–12} Only a minority of research-grade commercial UV–visible instruments provide a specialized lamp position for atomic penlamps that may be used to calibrate the wavelength axis of the optical spectrophotometer using spectral lines internationally recognized as secondary length standards.^{2,8,13,14}

* Corresponding author: (tel) 301-975-3935; (fax) 301-977-0587; (e-mail) David.Duewer@nist.gov.

[†] Chemical Science and Technology Laboratory, National Institute of Standards and Technology.

[‡] National Research Council Canada.

[§] Metals Division, Centro Nacional de Metrología.

^{||} Optical and Radiometric Division, Centro Nacional de Metrología.

[⊥] Physics Laboratory, National Institute of Standards and Technology.

- (1) ASTM E 925-83, Standard Practice for the Periodic Calibration of Narrow Band-Pass Spectrophotometers. In *Annual Book of ASTM Standards*, ASTM: West Conshohocken, PA, 2001; Vol. 03.06.
- (2) ASTM E 275-93, Standard Practice for Describing and Measuring Performance of Ultraviolet, Visible, and Near-Infrared Spectrophotometers. In *Annual Book of ASTM Standards*, ASTM: West Conshohocken, PA, 2001; Vol. 03.06.
- (3) Vinter, J. G. (revised by Knee, P.) In *Standards and Best Practice in Absorption Spectrometry*; Burgess, J. G., Frost, T., Eds.; Blackwell Science Ltd.: Oxford, U.K., 1999; Chapter 7.
- (4) Dodd, C. X.; West, T. W. *J. Opt. Soc. Am.* **1961**, *51*, 915–916.
- (5) Vandenbelt, J. M. *J. Opt. Soc. Am.* **1961**, *51*, 802–803.
- (6) Keegan, H. J.; Schleter, J. C.; Weidner, V. R. *J. Opt. Soc. Am.* **1961**, *51*, 1470.
- (7) McNeirney, J.; Slavin, W. *Appl. Opt.* **1962**, *1*, 365–367.

Low-mass fractions of holmium oxide (Ho_2O_3) in dilute acidic aqueous solution and in glass matrixes have been favored for use as wavelength calibration materials on the basis of spectral coverage and absorption band shape.^{4,6,10,12} Although band positions differ somewhat among qualitatively different matrixes, Ho_2O_3 band locations in solution and in various glasses are remarkably stable from one preparation to the next. Both aqueous and glass Ho_2O_3 reference materials are commercially available. Due to the sharper and less matrix-dependent bands provided by $\text{Ho}^{3+}(\text{aq})$ ions, the National Institute of Standards and Technology (NIST) of the United States and the Centro Nacional de Metrología (CENAM) of Mexico provide Certified Reference Materials (CRMs) for UV–visible wavelength calibration in the form of Ho_2O_3 in perchloric acid solution.^{15,16}

Recently, three National Metrology Institutes (NMIs) of the North American Cooperation in Metrology (NORAMET) of the Interamerican Metrology System evaluated the performance of these $\text{Ho}^{3+}(\text{aq})$ CRMs under “routine” operating conditions using commercial instrumentation. The study was not intended or designed to intercompare national wavelength scales. Rather, the goals were to (1) demonstrate comparability of wavelength measurements among the participants, (2) demonstrate the comparability between NIST and CENAM versions of CRMs, (3) acquire $\text{Ho}^{3+}(\text{aq})$ spectral data from a variety of spectrophotometers for use in a NIST study of wavelength-assignment algorithms, (4) provide a basis for a possible reassessment of the NIST-certified wavelength values, and (5) establish more realistic location uncertainties for these NIST certified values.

This paper reports the essential realization of the original goals through analysis of six data sets acquired in five laboratories of National Metrology Institutes. The results of this analysis support the efficacy of wavelength calibration using absorption-based wavelength standards in lieu of the traditionally preferred emission-based standards. That is, not only is calibration more convenient with absorption than with emission standards, it is more accurate. This surprising outcome was realized through the acquisition of densely sampled high-quality spectra, use of instruments that allow the true spectral slit width (SSW) to be set within 10% of nominal value, and use of a consistent definition of band location.

METHODS AND MATERIALS

Participants. The participating NORAMET laboratories were as follows: the Institute of National Measurement Standards (INMS) of the National Research Council (NRC) of Canada, the Metals Division (MD) and the Optical and Radiometric Division (ORD) of CENAM of Mexico, and the Chemical Science and

Table 1. UV–Visible Spectrophotometers in Study

participant	institution	instrument
CSTL	NIST	Perkin-Elmer Lambda 900
INMS	NRC	Perkin-Elmer Lambda 19
MD	CENAM	Varian Cary 5
ORD	CENAM	Perkin-Elmer Lambda 19
PL	NIST	Varian Cary 5e

Technology Laboratory (CSTL) and the Physics Laboratory (PL) of NIST of the United States. The study was coordinated by the Analytical Chemistry Division of CSTL.

Instrumentation. Each participant evaluated the study materials using a commercial spectrophotometer. The five instruments employed are described in Table 1. All instruments are at the high-performance end of commercially available products, as determined by production specifications and confirmed by experimental qualification procedures. Adaptations have been made in some cases to facilitate calibration of the wavelength axis of the instrument using appropriate atomic line emission sources.

Samples. Four samples were evaluated, two each of NIST Standard Reference Material (SRM) 2034 Holmium Oxide Solution Wavelength Standard from 240 to 640 nm^{11,16} and CENAM Reference Material DMR 41e Filtro de Óxido de Holmio.¹⁵ Both CRMs are 4% (mass fraction) Ho_2O_3 in 10% (volume fraction) perchloric acid, contained in a flame-sealed, nonfluorescent, fused-silica cuvette of high optical quality. The NIST samples are from the same 1999 batch preparation; the CENAM samples are from the same 2000 batch preparation. The samples were color-coded “blue”, “green”, “yellow”, and “red”. Figure 1 is a representative 0.1-nm SSW spectrum of these materials.

Protocol. Transmittance spectra from 230.0 to 679.9 nm with a data interval of 0.1 nm at SSWs of 0.1, 1.0, and 3.0 nm were requested for each sample. Spectra were to be collected in constant SSW (fixed-slit) mode using an air-path reference. The temperature of the sample at the time of measurement was to be determined to ± 0.5 °C. To enable assessment of components of variance in the spectral data, spectra for all samples at all SSW were to be collected in two separate sessions. Within each session, data were to be collected in the following order: red, green, blue, yellow. The two sessions were to be separated by an interval of at least 24 h. Participants were requested to specify the locations of 14 selected bands in each of the resulting 24 (4 samples \times 3 SSWs \times 2 sessions) spectra.

Instrumental wavelength and SSW accuracy were to be verified by the use of atomic emission lines.^{2,8,11–13,17} If necessary, wavelength was to be corrected using a low-order polynomial bias correction curve. The protocol distributed with the samples did not specify scan speed, response, or integration times.

- (8) Alman, D. H.; Billmeyer, F. W., Jr. *J. Chem. Educ.* **1975**, *52*, A315–A321.
- (9) Reule, A. G. *J. Res. Natl. Bur. Stand.* **1976**, *80A*, 609–624.
- (10) Weidner, V. R.; Mavrodineanu, R.; Mielenz, K. D.; Velapoldi, R. A.; Eckerle, K. L.; Adams, B. *J. Res. Natl. Bur. Stand.* **1985**, *90*, 115–125.
- (11) Venable, W. H., Jr.; Eckerle, K. L. *Didymium Glass Filters for Calibrating the Wavelength Scale of Spectrophotometers: SRM 2009, 2010, 2013, and 2014*; NBS Special Publication 260-66; U.S. Government Printing Office: Washington, DC, 1979. <http://ts.nist.gov/ts/htdocs/230/232/splist/splist.htm>.
- (12) Weidner, V. R.; Mavrodineanu, R.; Mielenz, K. D.; Velapoldi, R. A.; Eckerle, K. L.; Adams, B. *Holmium Oxide Solution Wavelength Standard from 240 to 640 nm: SRM 2034*; NBS Special Publication 260-102; U.S. Government Printing Office: Washington DC, 1986. <http://ts.nist.gov/ts/htdocs/230/232/splist/splist.htm>.

- (13) Kostkowski, H. J. *Reliable Spectroradiometry*; Spectroradiometry Consulting: La Plata, MD, 1997; Chapter 10 and Appendix F.
- (14) Sansonetti, C. J.; Salit, M. L.; Reader, J. *Appl. Opt.* **1996**, *35*, 74–77.
- (15) Reference Material DMR 41e; Centro Nacional de Metrología; 76900 Querétaro, México. <http://www.cenam.mx/sitio/MaterialesMetalicos.htm>.
- (16) Standard Reference Material SRM 2034; National Institute of Standards and Technology, Gaithersburg, MD. <http://srmscatalog.nist.gov/>.
- (17) ASTM E 958-93, Standard Practice for Measuring Practical Spectral Bandwidth of Ultraviolet–Visible Spectrophotometers. In *Annual Book of ASTM Standards*; ASTM: West Conshohocken PA, 2001; Vol. 03.06.

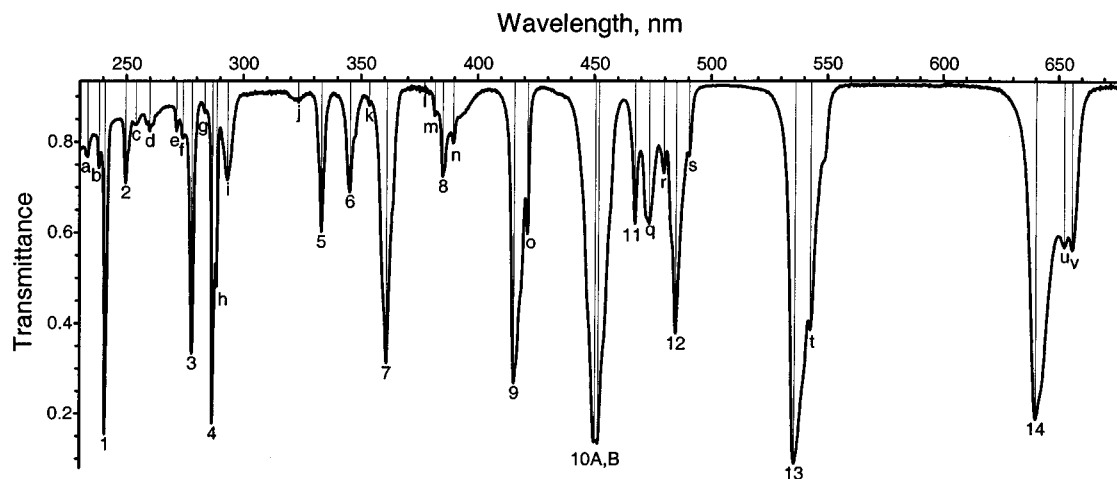


Figure 1. Representative 0.1-nm SSW UV-visible spectrum of 4% mass fraction Ho_2O_3 in 10% volume fraction perchloric acid. Bands having certified SRM 2034 and DMR 41 locations are labeled 1–14; the other spectral features evaluated are labeled a–v.

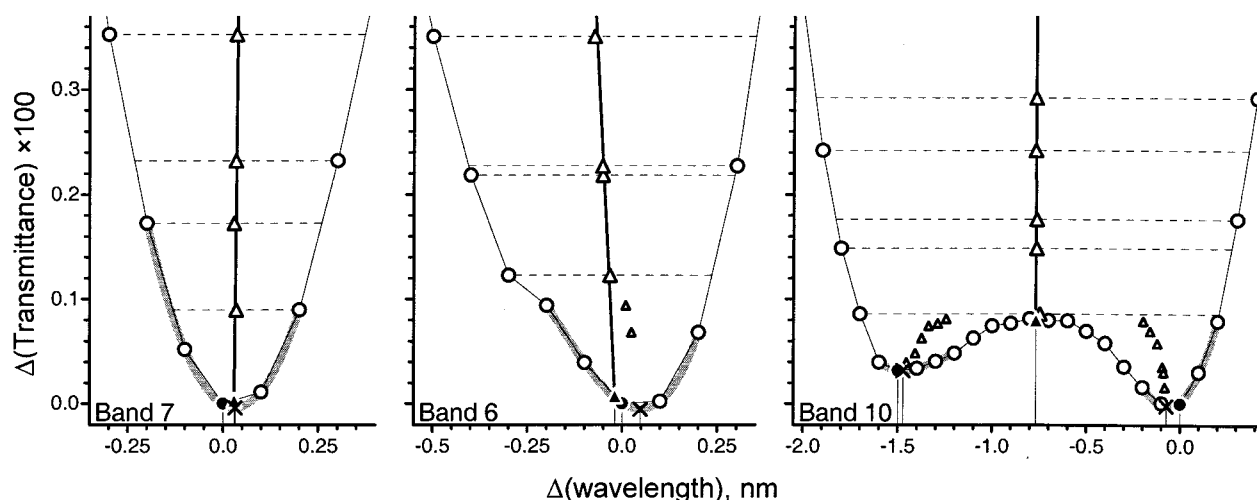


Figure 2. Band location estimation algorithms for three representative bands of a 0.1-nm SSW spectrum. These three graphical segments summarize representative data band-location calculations for the symmetric band 7 (left segment), the somewhat skewed band 6 (center), and the doublet of band 10 (right). The zero of the wavelength (horizontal) and the transmittance (vertical) axes in each segment is defined by the lowest-transmittance datum of each band. Observed data are denoted by open circles and are connected by a thin solid line; the local minimums (lowest observed transmittance) are denoted by closed circles. The cubic fit to the five data centered on each of the local minimums is represented by a thick gray line; the interpolated minimum (lowest calculated transmittance of the fitted curve) for each fit is denoted by the symbol \times . Representative bisector chords are represented as horizontal dashed lines; the chord midpoints are denoted with large open triangles. The band bisector defined by all “smoothly connected” midpoints within each segment is represented by the thick vertical line. The bisection minimum (the intersection of the band bisector and the band envelope) is denoted with a solid triangle. The small open triangles denote chord midpoints that were excluded from use in defining the band bisector. The thin vertical lines connect the variously defined band locations to the horizontal axis.

Protocol Exceptions. While all participants reported nominal measurement room temperatures of 22 °C, only INMS determined the actual temperature in the sample compartment (27.5 ± 0.5 °C). ORD/CENAM provided spectra at a data spacing of 0.12 nm. PL/NIST did not specify band locations for any spectrum. CSTL/NIST provided two sets of spectra, the first set acquired in June 2000 (before shipping samples to any other participant) and the second in June 2001 (after all other NORAMET participants returned data). The initial set, designated “CSTL1”, was inadvertently conducted using a light-starving 1:100 reference beam attenuation; the second, designated “CSTL2”, was conducted with no reference beam attenuation.

Band Location Algorithms. Figure 2 illustrates the three location algorithms that were evaluated: local minimum, inter-

polated minimum, and bisection. The center-of-gravity methods that work well with relatively broad bands^{18,19} are not well suited to the relatively “sharp” features of the UV-visible $\text{Ho}^{3+}(\text{aq})$ spectra. To ensure consistency, all feature locations were estimated at CSTL from spectra supplied by the participants, using special-purpose spreadsheet programs. When polynomial bias curves were specified, the wavelength values of all relevant spectra were corrected before estimating the band locations.

- (18) Cameron, D. G.; Kauppinen, J. K.; Moffat, J. K.; Mantsch, H. H. *Appl. Spectrosc.* **1982**, *36*, 245–250.
- (19) Zhu, C.; Hanssen, L. M. In *11th International Conference of Fourier Transform Spectrometry*; de Haseth, J. A., Ed.; AIP Proceedings 430; American Institute of Physics: New York, 1998; pp 491–494.

Local Minimum. The NORAMET protocol specified a data point spacing of 0.1 nm, regardless of SSW. While a more traditional data point spacing would have been 50%–100% of the SSW, the high data density permits defining band position as the wavelength location of the observed smallest (local) transmittance value. For “sharp” bands, where photometric noise near the minimum is negligible, this is a simple but robust algorithm with an intrinsic uncertainty of half of the point spacing. The open circles in Figure 2 denote the measured spectral data; the solid circles denote the local minimum locations.

Interpolated Minimum. A less granular estimate of band minimum location is provided by interpolating a smooth curve fit to data neighboring each local minimum. While commercial spectroscopic software seldom detail exact algorithms, most appear to use a polynomial fit of some form. The asymmetry of many of the bands in Figure 1 suggests use of a cubic or higher order polynomial where band location is defined as the root of the analytical first derivative of the interpolation polynomial that yields the smallest predicted transmittance. Cubic interpolation using the datum having the locally smallest transmittance, and the two data to each side reproduced within a few 0.001 nm the locations provided by INMS (quadratic) and CSTL (vendor proprietary). The thick gray lines in Figure 2 represent these cubic polynomial fits to each local minimum plus two data to each side; the location of the interpolated minimums are denoted with the symbol “x”.

Bisection. The certified band locations of NIST SRM 2034 were originally evaluated using a graphical bisection method most appropriate to instruments based on strip-chart recorders operating in a continuous scan mode.^{11,12} This method defines band location as the intersection of the band envelope with a “smooth” bisection curve that splits the band vertically “down the middle”. The bisection curve is defined using the midpoints of a series of horizontal chords that connect points of equal transmittance on each side of the band envelope. While dependent upon band-specific and somewhat subjective decisions regarding what chords to use and what constitutes a suitably “smooth” curve, a method suitable for digitized spectra was developed for comparative purposes.

The dashed lines in Figure 2 represent some of the chords used to define the bisectors; depending upon the band, up to 10 such chords may be used. Each chord is anchored on an observed datum and terminates in the interpolated band envelope of the opposite “wall”. The midpoints of these chords are denoted as large open triangles; midpoints that are judged to be insufficiently “smooth”ly continuous are denoted as small open triangles. The dark solid line denotes the linear estimate for the band bisector; the solid triangle denotes the intersection of the band bisector and the band envelope.

RESULTS AND DISCUSSION

Photometric Differences. The four samples can be distinguished by small but consistent differences in transmittance, especially in the UV range. These photometric signatures reflect small but fixed among-sample differences in $\text{Ho}^{3+}(\text{aq})$ concentration, trace impurities, and cuvette characteristics. The five spectrophotometers can also be distinguished by careful evaluation of the baseline, band resolution, and “noise” structure. For one instrument, the baseline characteristic of the spectra acquired in

the first session is quite different from that of the spectra acquired in the second session. The CSTL2 spectra are strikingly less “noisy” than are the (inadvertently attenuated) CSTL1 spectra. These among-instrument and among-session differences reflect differences in instrument parameter settings, optics, and data acquisition artifacts.

Bands Evaluated. In the 0.1-nm SSW $\text{Ho}^{3+}(\text{aq})$ spectrum of Figure 1, there are at least 36 transmittance minimums of at least 1-nm baseline width between 230 and 680 nm. While participants were requested to specify locations for only 14 of these, all of the identified minimums were post facto evaluated in all spectra acquired for this study. Several bands have sufficient “fine structure” with nearly equivalent transmittance minimums that a command to “find the smallest value within this window” does not always locate the same feature. Many of the less intense and wider bands are too sensitive to differences in photometric noise among the instruments for consistent characterization by the absolute local band minimum. Twenty-nine spectral minimums proved unambiguously present in all of the study’s 0.1-nm spectra. Since two of these minimums (for the band 10 doublet) are located within 1.5 nm of one another, all of these features can be visualized in 28 unique 2-nm-wide spectral “windows”. Figure 3 displays representative 0.1-, 1-, and 3-nm SSW spectra within these windows.

Many of the 29 minimums for the 0.1-nm spectra do not persevere to the larger spectral slit widths, although the 14 originally certified (numbered) bands do. The graphical evidence of Figure 3 is consistent with the theoretical ideal that represents the effect of SSW as the convolution of a triangular slit function—whose full width at half-maximum defines the SSW—with the high-resolution sample spectrum.²⁰ Such a model predicts the washing out of shoulder peaks and the fusion of doublets as is observed. Nevertheless, some of these spectral features do survive to larger SSW values.

Algorithm Differences. Figure 4 illustrates the distribution of the differences (mean bias \pm one standard deviation) among the three band location algorithms evaluated for all of the spectral features. The left-hand side of Figure 4 displays the biases between the local and the interpolated minimums. The mean bias for all bands for all SSW are much less than the 0.05 nm possible given the 0.1 data point spacing. This essential absence of observed bias may reflect averaging over five instruments whose wavelength axes are not identically registered. The bias distributions are consistent with the assignment of 0.03 nm as a “systematic error” component for band location in the original certification of SRM 2034.¹¹

The right-hand side of Figure 4 displays the biases between the bisector and interpolated minimum locations. Again, for most features, there is little difference; however, there are significant differences between the bisector and interpolated minimum algorithms for a few features. Band 10 is the most extreme case (see Figure 2), but other multimodal and asymmetric bands present problems as well. Band 10 demonstrates the definitional problem of the bisector method: it is easily defined for any given band but requires a subjective decision about where to start and stop bisection and how to extrapolate to the band envelope. The bisector algorithm is poorly suited to small shoulder features or

(20) Alman, D. H.; Billmeyer, F. W., Jr. *J. Chem. Educ.* **1975**, 52, A281–A290.

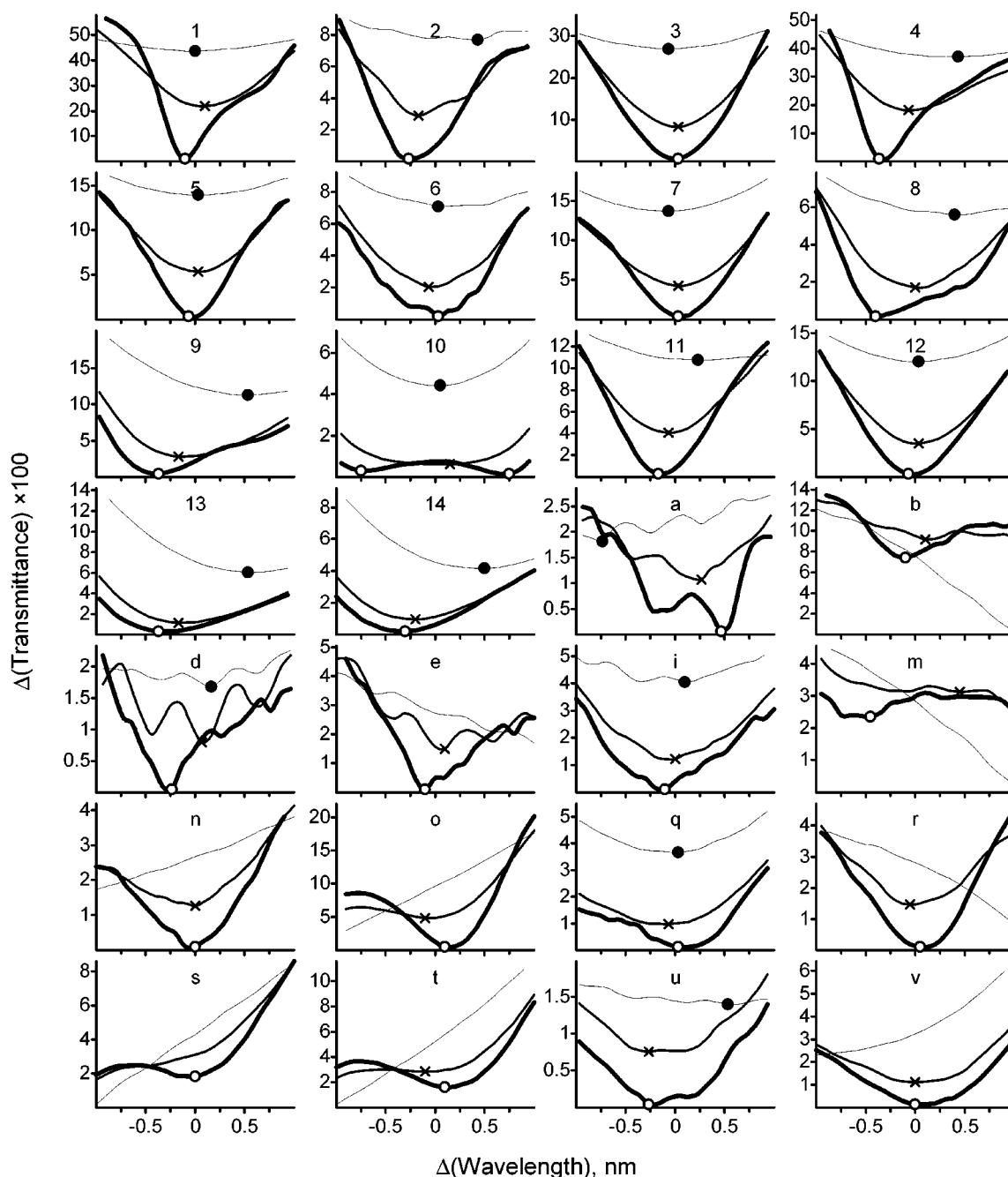


Figure 3. Representative spectral windows for the 29 features identified in all 0.1-nm SSW spectra acquired for this study. Each segment displays 0.1- (dark line, open circle), 1- (medium line, \times), and 3-nm (light line, solid circle) SSW spectra within a 2-nm wavelength window, where the symbols denote the location of transmittance band minima. The wavelength axis of each window is centered on the mean location of all the band minima displayed within the window; the transmittance axis of each window is scaled to the smallest and largest displayed transmittance.

to cases where the photometric noise approaches the magnitude of the transmittance gradient. On the other hand, the minimum and cubic interpolation methods both yield highly variable results when bands get very "flat", as happens with band 10 at a spectral slit width of 1 nm and as any shoulder band (such as most of the alphabetically labeled features) merges.

While the local and interpolated minimums are very similar with the very high data density spectra acquired for this study, the bias distributions between the bisector and interpolated minimum are somewhat smaller (both in magnitude and variability) than those between the bisector and local minimum (data

not shown). This suggests that the interpolated minimum is the better estimate for comparison with values certified using the bisection method. The interpolated minimum and bisection methods provide nearly identical location estimates for most features of interest in the $\text{Ho}^{3+}(\text{aq})$ spectra. For the few features that are differently located by the two methods, the variance properties of the different estimates are about the same. Since the cubic interpolation algorithm is identical or closely related to existing peak-location routines in many commercial packages, all further studies reported here utilize the interpolation minimum values.

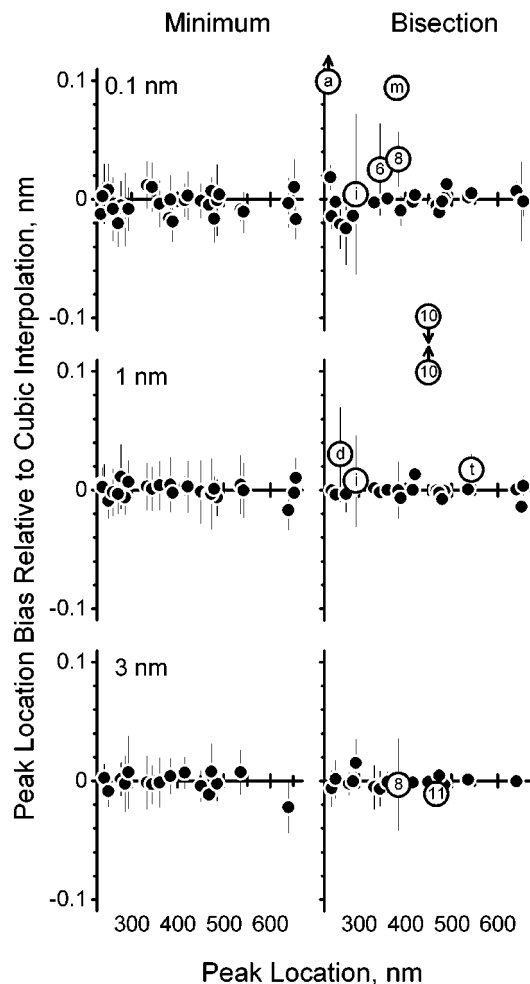


Figure 4. Relative biases among three definitions of band location. The three left-side segments display the location differences between the data and interpolated band minimums as functions of wavelength for all defined features of the 0.1-, 1-, and 3-nm SSW spectra. The three right-side segments likewise display the differences between the band bisection and the interpolated minimums. The solid circles denote the location difference observed for each spectrum acquired for this study, averaged over all spectra; the bars denote ± 1 standard deviation of the differences of all spectra. The open, labeled circles denote the features that yield the largest and most variable biases.

Components of Variance. The combined standard uncertainty^{21,22} for the position of a given feature is modeled as

$$u_c = \sqrt{u_{\text{replicate}}^2 + u_{\text{set}}^2 + u_{\text{sample}}^2} \quad (1)$$

The uncertainty component designated $u_{\text{replicate}}$ estimates the short-term replication variability, combining inter- and intrasession effects. It is estimated as the standard deviation of the differences between replicates:

$$u_{\text{replicate}} = \sqrt{\frac{\sum_{i=1}^{N_{\text{set}}} \sum_{j=1}^{N_{\text{sample}}} (X_{ij1} - X_{ij2})^2}{N_{\text{set}} N_{\text{sample}} - 1}} \quad (2)$$

where X_{ij1} and X_{ij2} are the interpolated minimum location estimates for the i th set of spectra for the j th sample in sessions 1 and 2.

The component designated u_{set} estimates the among-instrument variability and long-term operational differences for a given instrument. It is estimated as the standard deviation of the replicate average over the six sets (two from the CSTL, one each from the four other participants) of spectra, regarding the different samples as replicates of the same material:

$$u_{\text{set}} = \sqrt{\frac{\sum_{i=1}^{N_{\text{set}}} \left(\frac{\sum_{j=1}^{N_{\text{sample}}} (X_{ij1} + X_{ij2})/2}{N_{\text{sample}}} - \frac{\sum_{i=1}^{N_{\text{set}}} \sum_{j=1}^{N_{\text{sample}}} (X_{ij1} + X_{ij2})/2}{N_{\text{set}} N_{\text{sample}}} \right)^2}{N_{\text{set}} - 1}} \quad (3)$$

The component designated u_{sample} estimates the variability in band location among the four samples. It is estimated as the standard deviation of the within-set replicate averages, pooled over the six sets of spectra:

$$u_{\text{sample}} = \sqrt{\frac{\sum_{i=1}^{N_{\text{set}}} \left(\frac{\sum_{j=1}^{N_{\text{sample}}} (X_{ij1} + X_{ij2})/2}{N_{\text{sample}}} - \frac{\sum_{j=1}^{N_{\text{sample}}} (X_{ij1} + X_{ij2})/2}{N_{\text{sample}}} \right)^2}{N_{\text{set}} - 1}} \quad (4)$$

Figure 5 displays the three uncertainty components for all features. The u_{sample} is almost always smaller than $u_{\text{replicate}}$, indicating that the samples are statistically indistinguishable from each other with respect to measured band positions. In particular, the two samples furnished by CENAM provide indistinguishable band locations from those furnished by NIST. Another noteworthy feature of Figure 5 is that u_{set} dominates the other components. Table 2 reports the consensus mean location values and u_c for all of the features at each SSW; these values summarize just the measurements made for this NORAMET study and do not supersede certified values stipulated on CRM certificates. However, the u_{set} uncertainty components from this study have recently been incorporated into the band position uncertainties in the certificate for series 01 of NIST SRM 2034.

The variability among the data sets is elaborated in Figure 6. The three left-side segments display the location biases for each set relative to the consensus mean for the 0.1, 1, and 3 nm SSW spectra. Quadratic polynomial calibration curves of the measured biases to the consensus locations are defined by fitting the data for bands 1, 3, 5, 7, 9, 12, and 14. (These particular features were selected to provide a single set of spectral features appropriate to

(21) *Guide to the Expression of Uncertainty in Measurement*, 1st ed.; ISO: Geneva, Switzerland, 1993.

(22) Taylor, B. N.; Kuyatt, C. E. *Guidelines for Evaluating and Expressing the Uncertainty of NIST Measurement Results*; NIST Technical Note 1297; U.S. Government Printing Office: Washington, DC, 1994. <http://physics.nist.gov/Pubs/>.

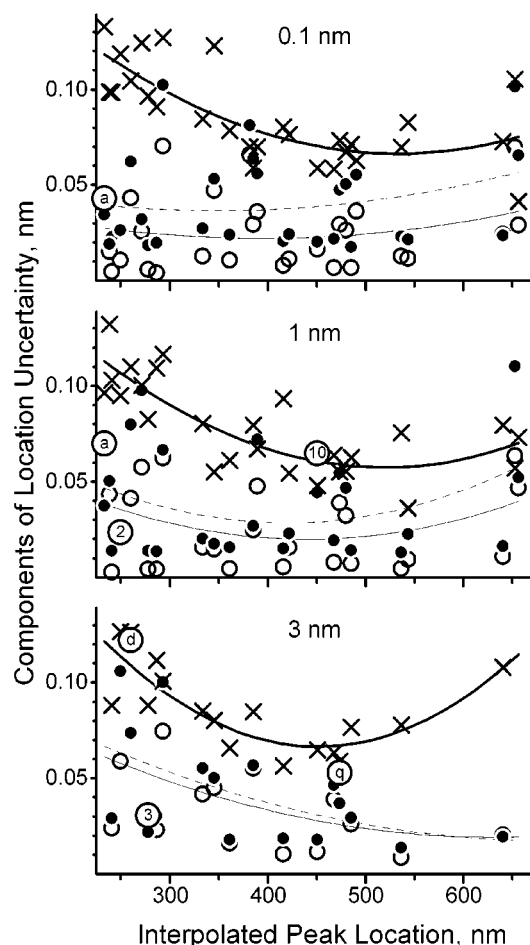


Figure 5. Estimates of uncertainty component for the interpolated minimum locations. The three segments display u_{sample} (open circles, light solid line), $u_{\text{replicate}}$ (solid circles, dashed line), and u_{set} (\times , dark solid line) as functions of location for all defined features of the 0.1-, 1-, and 3-nm SSW spectra. The larger labeled open circles denote features for which $u_{\text{sample}} > u_{\text{replicate}}$.

all three SSW settings that fairly uniformly covered the full wavelength range. No attempt was made to optimize feature choice; many other “reasonable” choices of feature number and identity provided similar calibration equations.) These relatively small but apparently systematic biases provide an estimate of the typical among-instrument wavelength-axis agreement achieved by calibration to emission line sources.

The three right-side segments of Figure 6 display the residual location biases after adjustment to the respective absorption band calibration curves. This calibration to $\text{Ho}^{3+}(\text{aq})$ spectral features dramatically improves the among-instrument wavelength-axis agreement.

CONCLUSIONS

The stated goals of the study are found to be satisfied. These goals are addressed individually:

(1) To Demonstrate Comparability of Wavelength Measurements among the Participants. Figure 6 demonstrates comparability within less than ± 0.2 nm at the 95% confidence level for the SSW range covered. This wavelength uncertainty range is at the outer limits of the overlap of the uncertainty of ± 0.1 nm for the CRM certification and the uncertainty of about ± 0.1 nm

Table 2. Spectral Feature Locations: Among-Set Means and Combined Standard Uncertainties (nm)

spectral feature	0.1 nm		1 nm		3 nm	
	mean	u_c	mean	u_c	mean	u_c
a	233.55	0.13	233.19	0.10		
b	238.39	0.10	238.57	0.13		
1	240.98	0.10	241.13	0.10	241.03	0.09
2	249.79	0.12	249.87	0.09	250.09	0.13
d	260.03	0.10	260.18	0.11	260.11	0.13
e	271.54	0.12	271.67	0.10		
3	278.17	0.10	278.13	0.08	278.07	0.09
4	287.03	0.09	287.23	0.11	287.62	0.11
i	293.35	0.13	293.39	0.12	293.38	0.10
5	333.49	0.08	333.49	0.08	333.47	0.09
6	345.52	0.12	345.39	0.06	345.50	0.08
7	361.29	0.08	361.25	0.06	361.11	0.07
m	381.97	0.07	382.25	0.14		
8	385.37	0.06	385.62	0.08	386.01	0.08
n	389.85	0.07	389.75	0.07		
9	416.04	0.08	416.26	0.09	416.88	0.06
o	421.78	0.08	421.57	0.05		
10A	450.60	0.06				
10			451.42	0.05	451.26	0.06
10B	452.00	0.07				
11	467.77	0.06	467.80	0.06	468.10	0.06
q	473.73	0.07	473.54	0.06	473.55	0.06
r	479.97	0.07	479.90	0.06		
12	485.20	0.07	485.21	0.06	485.17	0.08
s	490.72	0.06				
13	536.43	0.07	536.55	0.08	537.21	0.08
t	543.30	0.08	543.06	0.04		
14	640.43	0.07	640.48	0.08	641.09	0.11
u	652.69	0.11	652.68	0.06	653.08	0.25
v	656.14	0.04	656.09	0.07		

asserted as the measurement accuracy by each participant, supporting a recommendation for reevaluating the uncertainties of SRM 2034 (see below).

(2) To Demonstrate the Comparability between NIST and CENAM CRMs. Despite discernible differences in peak and baseline transmittance among the two NIST samples and the two CENAM samples, Figure 5 demonstrates that the uncertainty component attributable to sample differences is less than that attributed to simple replication and that attributed to differences among instruments. This finding demonstrates the robustness of peak wavelength determination with respect to spectral differences due to concentration, cell conditions, and contamination. We believe that dilute acidic Ho_2O_3 solution is a candidate for an intrinsic standard material for UV–visible wavelength calibration.²³

(3) To Evaluate Wavelength Assignment Algorithms. For the data density of 0.1 nm/data point, as used here, the data of Figure 4 support the adequacy of a local cubic fit interpolation of the peak minimum. This algorithm is functionally equivalent to most commercial peak location computer algorithms that report locations to a finer granularity than the sampling grid. Such methods may be expected to perform well at reduced data densities, but this claim cannot be supported by the present study. A computer implementation of the band bisection method employed in the original NIST certification of SRM 2034 was found

(23) ANSI/NCSL Z540.1-1994, *American National Standard for Calibration, Calibration Laboratories and Measuring and Test Equipment, General requirements, 1st ed.*; American National Standards Institute (ANSI)/National Conference of Standards Laboratories (NCSL), August 1994; p 7. <http://global.ihc.com/>.

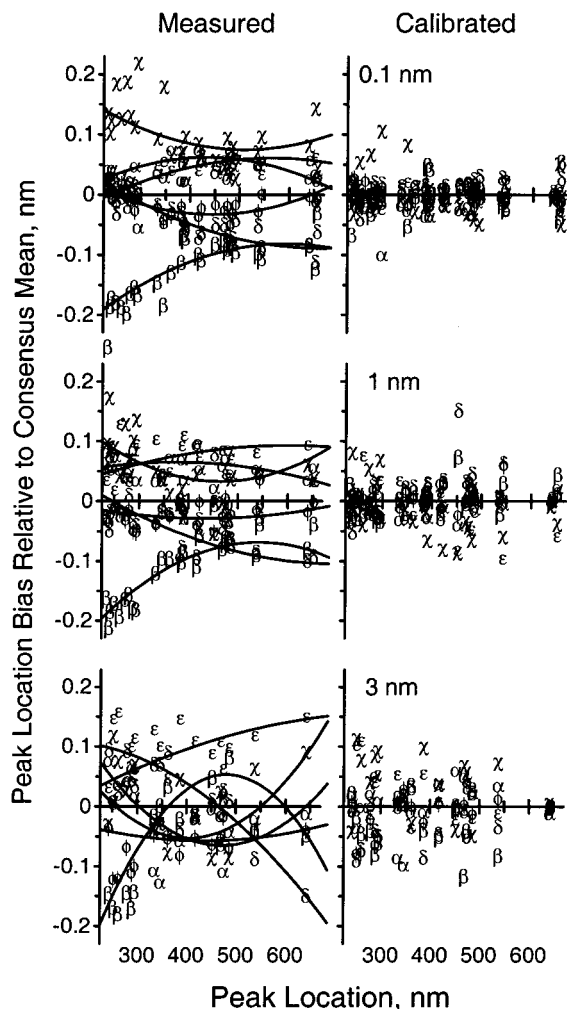


Figure 6. Relative location biases. The three left-side segments display location bias measured for each set relative to the consensus mean for the 0.1-, 1-, and 3-nm SSW spectra. At each SSW, biases are estimated as the interpolated location difference averaged over all spectra acquired at that SSW. Quadratic polynomial calibration curves of the measured biases to the consensus locations are also displayed. Each different Greek symbol denotes results for one of the six data sets. The three segments to the right display the residual bias data after quadratic calibration.

to yield significant departures from the interpolated local minimum for certain bands and SSWs. This performance supports the anecdotal observation that the method suffers from definitional subjectivity, as illustrated in Figure 2 for bands 6 and 10.

(4) To Assess the Adequacy of the Certified Values of SRM 2034. The consensus mean values for the locations of bands 1–14 listed in Table 2 agree with the certified values for SRM 2034 within a tolerance defined by the overlap of the 0.1-nm uncertainty originally quoted for SRM 2034 and the 95% uncertainty bounds of the present data. Nevertheless, the inadequacies of the originally used bisection location algorithm demonstrated

in Figure 4 suggest the advisability of a revaluation of the certified positions for SRM 2034, series 02, to be produced in the year 2002. The value assignment should involve comparative measurements on different instruments and may include some of the present data. A more obvious need than revaluation of the positions is that for revaluation of the uncertainties. This assessment is not intended as a judgment on the scientific quality of the original work but as a recognition of technological changes that favor a computer-oriented peak-location algorithm and as a response to recent uncertainty guidelines.^{21,22}

(5) To Establish Realistic Location Uncertainties. The present study illustrates that calibration uncertainty across different instruments operated by skilled operators should be included in the uncertainty analysis. The results of this study have already been incorporated in the quoted uncertainties for SRM 2034, series 01, produced in 2001.¹⁶ The redesigned table of certified values associates a separately computed uncertainty with each certified band position for each SSW. The majority of these uncertainties exceed the blanket value of 0.1 nm assigned to all bands and SSWs for previous series. The stated comparability of all series of the SRM for the useful life of 10 years implies that the new uncertainties may be applied to prior series of SRM 2034 for a period ending on December 31 of the 10th anniversary year of the filter (for which the series is the last two digits of the production year).

An unexpected conclusion that may be drawn from Figure 6 is that the consistency of wavelength calibration among instruments may be *improved* by the use of $\text{Ho}^{3+}(\text{aq})$ absorption standards over the use of atomic emission lines. Contributing factors may include instrument calibration protocol differences, dependence of the emission calibration on alignment of the lamp, and asymmetric slit functions. It may be that broad absorption peaks improve calibration consistency for SSW of 0.1 nm or greater by minimizing the influence of slit function asymmetry. In any case, the use of an absorbing standard ensures that the optical axis of importance is the same for calibration as it is for applications.

ACKNOWLEDGMENT

Certain commercial materials, instruments, software, and equipment are identified in this paper to specify the experimental procedure as completely as possible. In no case does such identification imply a recommendation or endorsement by the Centro Nacional de Metrología, the National Institute of Standards and Technology, or the National Research Council Canada; nor does it imply that the material, instrument, software, or equipment is necessarily the best available for the purpose.

Received for review February 7, 2002. Accepted April 25, 2002.

AC0255680